



RESEARCH ARTICLE

Modelling outlet power loss in Archimedes screw generators

Scott C. Simmons^{1,*}  and William David Lubitz^{1,†} 

¹School of Engineering, University of Guelph, 50 Stone Rd E, Guelph, ON N1G 2W1, Canada

*Corresponding author. E-mail: ssimmons@uoguelph.ca

†These authors contributed equally to this work.

Received: 13 May 2024; **Revised:** 13 September 2024; **Accepted:** 12 October 2024

Keywords: Archimedes screw generator; hydropower; power loss; modelling; renewable energy

Abstract

Archimedes screw generators are a small-scale, eco-friendly hydropower technology. Despite their promise as a sustainable energy technology, the design specifics of the technology are not well documented in the published literature. Existing performance prediction models often fail to accurately forecast power loss, particularly as it relates to the outlet of the screw generator. To address this, a comprehensive computational fluid dynamic model was developed and evaluated using both laboratory-scale experiments and real-world data. This yielded an extensive dataset that covered wide variations in design parameters. The dataset was then used to inform the development and evaluation of an outlet power loss prediction model. The resulting model significantly improved the accuracy of overall performance predictions, reducing average error to 13.68 % compared with nominal experimental data – a substantial improvement over previous models, which averaged around 42.55 % error for the same test cases. Notably, the new model achieved an absolute error of 5 % or less in over 26 % of comparison points, marking a remarkable advancement by predicting outlet power loss by more than 28.8 %.

Impact Statement

When properly designed, Archimedes screw generators are an efficient, fish-friendly, eco-friendly sustainable energy solution. They are capable of operating effectively under a wide range of conditions and schemes. They have been shown to be very efficient when operating at low heads and moderate flow rates; ranges that are not commonly occupied efficiently by other hydropower technologies. However, their design is not well documented in the literature. This paper presents a model that offers a significant improvement to state-of-the-art design and performance predictions in Archimedes screw generators. When integrated into a full performance model, this outlet power loss model is able to substantially improve overall prediction accuracy, and consequently improve design optimization of the technology.

1. Introduction

This paper outlines the design, development and evaluation of a power loss prediction model for outlet power loss in Archimedes screw generators (ASGs). The model was able to improve overall ASG powerplant performance predictions when implemented as a module in full performance prediction software.

An ASG is a micro-hydropower technology often used at sites with low heads and moderate flow rates to convert hydraulic power into rotation mechanical power. Archimedes screw generators are

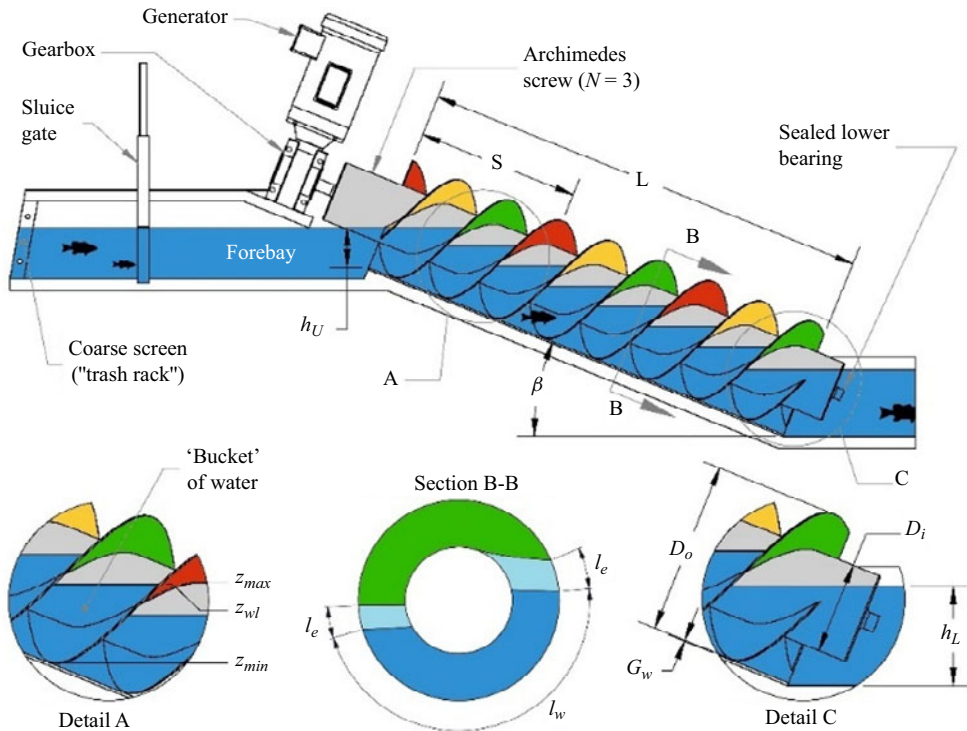


Figure 1. Simplified ASG powerplant layout. Parameters used to quantify filling levels of screw buckets are shown in Detail A, parameters used to describe gap leakage are shown in Section B and the outlet water level and gap width are magnified in Detail C.

commonly installed in run-of-river schemes, which contributes to its reputation as an eco-friendly hydropower technology (Simmons & Lubitz 2021). Powerplants using ASGs often operate with river-to-wire efficiencies of approximately 75%; however, some screw generator powerplants operate more efficiently (Fergnani, Silva & Bavera 2017).

Archimedes screws have a simple, robust design in comparison with other hydropower technologies. They are made up of a helical array of blades that are fixed along a central, cylindrical tube. In its most common orientation, the screw is held between bearings and rotates within a fixed trough. With some exceptions, screws most commonly have three or four blades. A small intentional gap exists between the blade tips and the fixed trough. Although the gap introduces a phenomenon called ‘gap leakage’ flow (Q_g) into the system, it improves mechanical performance by reducing friction and preventing wearing of the blades and trough.

The screw is connected to a generator at the top of the screw via a gearbox. Screw generators usually operate at low speeds (between 10 and 80 rev min⁻¹), so a gearbox is required to convert rotation speed to a speed more suitable for a standard electrical generator. Larger screws tend to operate more effectively at lower rotation speeds. The generator is used to convert rotational mechanical energy into electricity for on- or off-grid use. The layout of a common ASG installation is shown in figure 1 with annotations to indicate variables and operating parameters.

Archimedes screws are often described geometrically by their outer diameter (D_o), inclination angle (β) and number of blades (N). Dimensionless design ratios are often employed to fully define the geometry of a screw generator. The diameter ratio is the ratio between the inner and outer diameters of the screw (D_i/D_o). The pitch ratio is the ratio between the screw pitch and the outer diameter (S/D_o). Lastly, the length ratio is the ratio between the flighted length of the screw and the pitch (L/S).

During operation, water enters the screw at a known upper water level (h_U) and flow rate (Q). The screw rotates at a given speed (ω), allowing water to enter between its blades. Water enters the space between the screw blades. Once the blades fully enclose the volume of water, that volume of water is described as a 'bucket' of water (Rorres 2000). The water level within each bucket (z_{wl}) depends on the flow, rotation speed and geometry of the screw. Buckets are formed and travel along the length of the screw within chutes. Chute is the term used to describe the volume between two adjacent blades. For example, all the buckets formed between the green and red blades of figure 1 would be within the same chute.

Buckets are usually described by the dimensionless bucket fill height ratio (f), which is calculated as

$$f = \frac{z_{wl} - z_{min}}{z_{max} - z_{min}}, \quad (1.1)$$

where z_{min} is the minimum water level of a bucket and z_{max} is the maximum water level before water overtops the inner cylinder and spills into the next successive bucket along the chute.

The flow of water overtopping the inner cylinder is called overflow leakage (Q_o). Overflow leakage occurs when the bucket fill height ratio is $f > 1$. When $f = 1$, the buckets are as full as they can be without experiencing overflow leakage. When $f < 1$, the buckets are underfilled and only experience leakage losses in the form of gap leakage. When an ASG has underfilled buckets, it tends to operate with less energetic efficiency. Power conversion is largely due to hydrostatic pressure differences between the screw buckets. Generally, dynamic pressure has a proportionally very small effect on screw performance (Simmons & Lubitz 2020).

Archimedes screws have been used for pumping since roughly the 7th century BCE (Dalley & Oleson 2003). It appears that their development has been influenced by many generations of experience-based design and heuristic modelling. In turn, screw generator design appears to be largely experience based and empirical as well. Until recently, screw generator design methods in the published literature did not yield site-optimized designs. The main goal of the authors' research is to develop tools that optimize site-specific ASG design and improve return on investment, energetic efficiencies or a combination of both.

When considering the performance of an ASG, the net mechanical power output is described with the following equation:

$$P = P_s - P_{L,f} - P_{L,o}. \quad (1.2)$$

In the equation, the net mechanical power (P) is equal to the ideal shaft power (P_s), minus the frictional power loss ($P_{L,f}$) and outlet power loss ($P_{L,o}$). The ideal shaft power is the total frictionless mechanical power that the screw blades convert from water pressures within the screw buckets. The frictional power loss describes the viscous pressure effects in the system; for example, an increasing rotation speed can increase the wall shear stress and its associated frictional power loss. Finally, the outlet loss, which is the focus of this study, is the loss incurred as water exits the lower end of the screw into a channel or reservoir at a given lower water level (h_L).

The total flow rate (Q) also describes the net performance of an ASG. Screw generator efficiency is impacted by leakage losses during operation. The total flow rate through an ASG is

$$Q = Q_b + Q_g + Q_o, \quad (1.3)$$

where Q_g is the gap leakage flow rate, Q_o is the overflow leakage rate and Q_b is the bucket flow rate. The bucket flow rate is directly associated with power production, while the leakage flow rates are directly associated with power loss.

To optimize the design of an ASG powerplant, accurate prediction models for all components of power and flow are required. With accurate modelling, optimization software can be used to run through design iterations and determine the best geometry and configuration for a powerplant with the goal of achieving the highest mechanical or economic efficiency.

In general, current performance prediction models in the literature lack accuracy. More modern models are based on laboratory-scale experimental data on screws with small diameters ($D_o = 0.15$ to 0.38 m). So, these models have not been robustly proven to accurately predict performance of large, real-scale screw generator installations (i.e. $D_o = 0.6$ to 5.0 m).

Prediction models for power production are present in the published literature (Lubitz, Lyons & Simmons 2014; Nuernbergk 2020). One of the models was developed empirically based on data gathered from a range of laboratory experiments and field measurements (Nuernbergk 2020). It predicts mechanical efficiency based on experimental evidence, then uses efficiency and available hydraulic power to predict power production. The other model uses a first-principles approach to predict screw generator performance and was validated with laboratory-scale experimentation (Lubitz *et al.* 2014). The model uses flow, water levels and screw geometry to compute bucket fill heights. Then, using the fill height, integrates along a finely meshed representation of a screw blade to find hydrostatic pressure and consequently torque conversion during screw operation. Power loss models are also present in the model; they include a frictional power loss model that was similarly developed from first principles (Kozyn & Lubitz 2017).

There are some models in the published literature that predict components of a screw outlet. Current gap leakage models were developed from first principles using basic fluid mechanics concepts (Lubitz *et al.* 2014; Nuernbergk 2020). Data from a more recent study suggest there is room to improve these models (Simmons & Lubitz 2020). An empirical update to the gap leakage model presented by Lubitz (2014) was posed; it demonstrated accuracy improvements to predictions by an average of 14.3 % across all scale sizes of screw generator installations (i.e. $D_o = 0.15$ to 5 m) (Simmons & Lubitz 2022).

Overflow leakage rates were also modelled using a first-principles approach (Aigner 2008; Nuernbergk & Rorres 2013; Kozyn & Lubitz 2017; Nuernbergk 2020); however, the resulting model was shown to lack accuracy, and an empirical correction was applied (Songin & Lubitz 2019). The correction relationship was exclusively informed by laboratory-scale experimental data and there are some indications that the model may be less accurate for large-scale screw generators.

Power loss associated with the outlet of screw generators has also been modelled the literature (Kozyn & Lubitz 2017; Nuernbergk 2020). The outlet is located at the lower end of a screw generator. At the outlet, water drawings from the final buckets into a lower reservoir, basin, or channel. Recent computational fluid dynamic (CFD) analysis and field measurements taken at full-scale ASG powerplants have suggested that current outlet loss models in the literature lack accuracy in full-scale screw installations (Simmons *et al.* 2021).

The Kozyn (2016) model separated outlet power loss into two components to make analysis easier (Kozyn & Lubitz 2017). The outlet power loss was described as a function of losses due to submersion, and hydraulic losses due to expansion into the lower basin. The outlet expansion loss was described as the power loss associated with the changing cross-sectional geometry as water exited the screw into a reservoir or channel. Outlet expansion loss was modelled using the principles of Borda–Carnot head loss (Kozyn & Lubitz 2017). Outlet submersion loss was more complicated; it related to the concepts of an optimal lower water level. For improved mechanical efficiency, the lower water level must be set at a screw-specific optimal height. Nuernbergk proposed the following geometric relationship to define the optimal lower water level (Nuernbergk 2020):

$$h'_L = \frac{D_o + D_i}{2} \sqrt{1 - \left(\frac{S \tan \beta}{\pi D_o}\right)^2} \cos \beta - \frac{S}{N} \sin \beta. \quad (1.4)$$

Figure 2 shows an illustration of a screw set to its optimal lower water level.

The lower water level is often described in dimensionless terms as the lower submergence (ψ_L)

$$\psi_L = \frac{h_L}{D_o \cos \beta}. \quad (1.5)$$

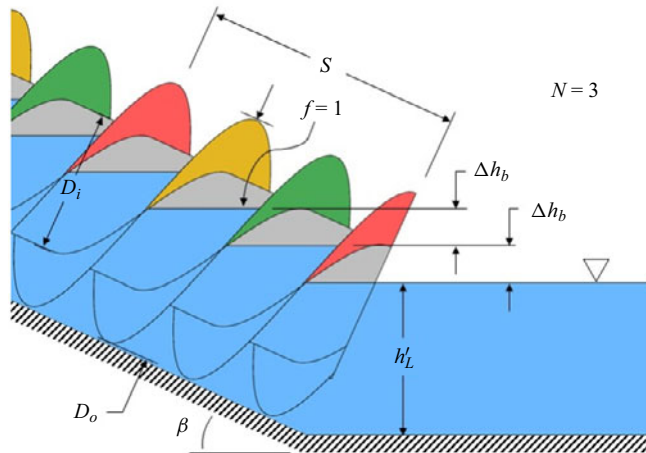


Figure 2. Optimal lower water level and the parameters used by Nuernbergk (2020) to define it.

Correspondingly, the optimal lower submergence is

$$\psi'_L = \frac{h'_L}{D_o \cos \beta}. \quad (1.6)$$

The optimal outlet submergence provides the screw with an amount of backpressure that helps the final buckets drain more effectively. When the lower water level is too high (i.e. $\psi_L > \psi'_L$), the screw outlet becomes flooded. Under this condition, water will flood back into the last buckets of the screw from the lower basin or reservoir and begin to counteract the power generator capabilities of the last buckets. When the lower water level is below optimal (i.e. $\psi_L < \psi'_L$), the final buckets of the screw drain prematurely since the backpressure at the outlet is not sufficient. There exists an optimal lower water level (ψ'_L) where the power losses associated with back flooding and premature drainage are minimized (Nuernbergk 2020). The optimal lower water level is very screw-dependent; it is based on the geometry of a screw generator installation. However, in the most common ASG orientation, the optimal submergence is roughly $\psi_L \approx 0.60$ (i.e. the outlet is approximately 60 % submerged) (Nuernbergk 2020).

Considering all models used for performance predictions in ASGs, the authors have determined that the outlet loss models require the most immediate attention. Outlet water levels can vary widely at screw generator installations; there are large seasonal variations in outlet water levels, and one unique installation was subject to tidal variations (Simmons *et al.* 2021). Varying low and high water levels at a screw outlet has been observed to significantly impact screw generator performance (Kozyn & Lubitz 2017; Simmons *et al.* 2021) – the existing methods to model these impacts are limited. The focus of this study is to address these limitations and present an improved outlet power loss model that could be implemented to make overall power predictions more accurate in design optimization. Additionally, the relationship for the optimal lower water level that Nuernbergk proposed (i.e. (1.4)) is only valid when the screw buckets are full, but not overflowing (i.e. $f = 1$). So, one goal of the model proposed by the authors in this study is to suggest improvements that have validity across all practical fill heights.

2. Methodology

Until recently, there has been a lack of comprehensive large-scale screw generator performance data in the literature. To address this issue, laboratory experimentation and field measurements were conducted to quantify ASG performance across a range of scale sizes (Simmons *et al.* 2021). Since it is difficult to vary input parameters in an operating screw generator powerplant, only a few high-quality datapoints were collected for large-scale ASG performance. So, the laboratory and field data were collected to inform the design of a CFD model. The CFD model was evaluated across a wide range of scale-sized

Table 1. Three different scale-sized laboratory screw generator datapoints used for the evaluation of numerical simulations.

Screw name	D_o (m)	D_i (m)	S (m)	L (m)	N (-)	B ($^\circ$)	ω (rad s $^{-1}$)	Q (m 3 s $^{-1}$)	P_{exp} (kW)
Lab Screw A	0.150	0.078	0.150	0.600	3	24.9	6.28	0.001	0.0021
Lab Screw 2	0.316	0.168	0.318	1.219	3	24.5	5.24	0.008	0.0299
Lab Screw 15	0.381	0.168	0.381	0.617	4	24.5	3.36	0.01	0.0224

Table 2. Representative datapoints from field measurement campaign.

Screw name	D_o (m)	D_i (m)	S (m)	L (m)	N (-)	B ($^\circ$)	ω (rad s $^{-1}$)	Q (m 3 s $^{-1}$)	P_{exp} (kW)
Waterford	1.390	0.762	1.390	4.538	3	22	4.26	0.462	7.386
Buckfast	2.500	1.220	2.500	10.562	4	26	3.01	2.095	92.88
Ruswarp	2.900	1.200	3.070	5.117	3	22	2.80	3.754	32.50
Ferrara	3.600	1.800	4.300	7.400	3	22	2.34	5.030	133.35

screw data so that it could be reasonably run with any combination of geometry or operating parameters (within the evaluated range) to produce accurate approximations of screw generator performance. Data from the laboratory, field measurements and CFD simulations were used to inform the development of an improved outlet power loss model. Data from each source were also used to evaluate the outlet power loss model.

2.1. Laboratory experiments

Laboratory experiments were conducted in the University of Guelph's Archimedes Screw Laboratory. To collect a datapoint, the pump was set to a desired system flow rate, and the the motor's variable frequency drive was set for a desired screw rotation speed. The system was allowed time to equilibrate; at equilibrium, the average water levels in each basin remained constant. At this point, datalogging software was run to collect 60 s of sensor readings. Due to the nature of filling and emptying buckets, screw torque and water levels have slight oscillations during normal operation. So, the 60 s sensor readings were time averaged to better characterize the performance of the screw generator.

Three different laboratory screws were used to evaluate the CFD model, they varied by scale size. The geometry, nominal flow rate and measured power for characteristic run points are shown in table 1.

More detailed information about the collection of each datapoint of table 1 can be found in the literature. This apparatus was used to collect data for Lab Screw 2 (Kozyn 2016) and Lab Screw 15 (Simmons 2018). A similar but smaller apparatus was used in the same laboratory to conduct experiments on Lab Screw A (Lyons 2014).

2.2. Field measurements

It is very difficult to gather data from an operational ASG powerplant that is both high quality and has enough detail to be useful for model evaluation and development. To gather a useful, high-quality datapoint that describes screw generator performance, the flow rate, water levels, torque (or generated power) and rotation speed must be quantified. It is specifically the flow rate and torque that are most difficult to gather in an operating powerplant; usually neither are directly measured, but rather estimated based on other measurements. Table 2 shows the dimensions, operating parameters and electrical power production of each site.

For all four powerplants, measurements of electrical power, rotation speed and water levels were either readily available or straightforward to gather while on site. Flow rate data were much more difficult to gather. Each site had unique characteristics that called for unique solutions to quantify flow

Table 3. Simulated screw dimensions and operating parameters. All screws have the same design ratios (i.e. D_i/D_o , S/D_o , S/L).

Screw number	Scale	D_o (m)	D_i (m)	S (m)	L (m)	N (-)	B ($^\circ$)	G_w (m)	ω (rad s $^{-1}$)	Q (m 3 s $^{-1}$)
1	0.47	0.148	0.079	0.149	0.572	3	24.5	0.002	6.02	0.00115
2	1	0.316	0.168	0.318	1.220	3	24.5	0.002	5.24	0.00827
3	2.13	0.675	0.359	0.678	2.600	3	24.5	0.004	4.69	0.0699
4	3.16	1.000	0.532	1.000	3.860	3	24.5	0.006	4.19	0.202
5	6.33	2.000	1.060	2.010	7.710	3	24.5	0.008	3.30	1.23
6	11.1	3.500	1.860	3.510	13.500	3	24.5	0.010	2.27	4.51
7	15.8	5.000	2.660	5.020	19.300	3	24.5	0.010	1.79	10.3

rate. Further details regarding the set-up and data collection can be found in the supplementary material available at <https://doi.org/10.1017/flo.2024.29>, or in the literature (Simmons *et al.* 2021).

2.3. Numerical simulations

A transient, two-phase, dynamically meshed, three-dimensional CFD model of an ASG was developed with OpenFOAM (v4.0, The OpenFOAM Foundation). The model was developed to accurately approximate screw generator behaviour across a wide range of geometries and operating conditions. Model details, grid sensitivity and evaluation are shown in the supplementary material, and further details can be found in the literature (Simmons *et al.* 2021; Simmons, Dellinger & Lubitz 2023).

The simulation results had reasonable agreement with the experimental and field measurements, suggesting that the CFD model can be used as an accurate approximation of operating ASGs. To take advantage of the CFD model's ability to approximate screw performance across a wide range of scale sizes and configurations, sets of simulations were run for seven different scale-sized screw generators (cf. table 3) representing a range from pico- to small-scale hydropower sites.

The geometry of the simulated screws was based on the most tested laboratory-scale screw at the University of Guelph's Archimedes Screw Laboratory. The seven scales were selected to represent the full range of ASGs. Screw 2 in table 3 is identical to the most tested laboratory-scale screw. Screw 1 represents the scale size of the smallest laboratory screw in the Archimedes Screw Laboratory. Screws 3 to 6 roughly match the scale of the screws in the field studies. And screw 7 is the scale of the largest operating screw at time of publication (Simmons *et al.* 2021). Though the simulations varied in length scale, they were otherwise geometrically identical; all screws had the same design ratios (i.e. D_i/D_o , S/D_o , S/L), proportions and inclination angles. Keeping proportions constant allowed for direct comparisons of performance against length scale.

All screws operated with fill ratios of $f = 1$, and outlet submergence was varied. To be computationally economical, outlet submergence was varied from $\psi_L = 0.1$ to 1.0 by increments of 0.1 for screw 2 and screw 5. Screw 2 was selected since it represents the real laboratory screw, and screw 5 was selected since it represents the length scale of a standard operating ASG. After running simulations on screws 2 and 5, a preliminary analysis was conducted. Results of the preliminary analysis suggested that the remaining screws (screws 1, 3, 4, 6 and 7) could be simulated with submergence levels of $\psi_L = 0.2, 0.5, 0.6$ and 0.7 while still capturing the main trends observed in the preliminary data.

3. Data and model development

This section outlines analysis of the initial data as well as the development of the new outlet power loss model, correction terms and an evaluation of the new model with comparisons with the current state-of-the-art outlet power loss model.

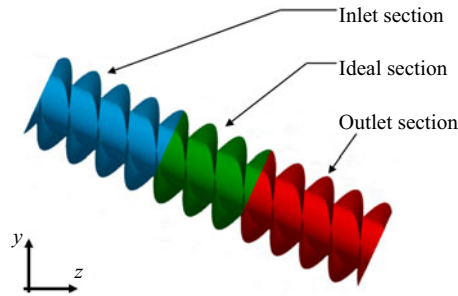


Figure 3. Three sections of simulated screw domain: inlet section, ideal section and outlet section.

3.1. Initial data and analysis

Numerical simulations yielded two components that were dimensionally homogeneous to pressure: static pressure distribution and viscous drag. To determine total mechanical torque on the simulated screws, the two terms were integrated over all submerged surfaces yielding component forces. The resultant forces were taken as a moment about the screw axis of rotation. To find the torque contribution due to hydrostatic pressure (the ‘power-producing torque’) and the torque component that represents frictional power loss. To determine the net mechanical torque at the screw shaft, the difference of the two components is found.

Since it is difficult to directly measure outlet effects, the simulation domain was split into three sections corresponding to [figure 3](#) (the inlet section, ideal section and outlet section).

A bucket of the screw requires one full pitch length to form, so the ideal section was selected as one pitch length at the longitudinal centre of the screw. The inlet and outlet section were set as the remaining segments of screw at their respective inlet or outlet ends of the screw. Theoretically, in a very long Archimedes screw, the buckets at the longitudinal centre should operate with negligible impact on the inlet or outlet of the screw; they would be operating in an ideal, undisturbed state. The ideal bucket is a great characteristic representation of an Archimedes screw; many models use an idealized bucket to calculate the ideal power-producing torque, then use power loss models to subtract of system loss estimates.

Screws tested in this study had a length ratio of approximately 4.2, meaning that the screw is approximately 4.2 pitch lengths long. This is relatively long for an Archimedes screw, so the ideal section should be less impacted from the inlet and outlet, respectively. To quantify the loss, mechanical power and its components were calculated for each section of the screw. [Figure 4](#) demonstrates the power and power components as panels for each section of screw 2 across the full range of outlet submergence levels. In the figure, power is shown as a static pressure component (P_p , left) and viscous pressure component (P_v , centre) alongside the resultant power (P , right). Each panel has curves representing the inlet, ideal and outlet sections as well as the full screw, and the idealized full screw power. The idealized full screw power was found by scaling the ideal section power to the full screw length with the length ratio; it represents the power that an ASG would produce were it not subject to inlet or outlet effects and if both the top and bottom of the screw were immersed at ideal, nominal levels.

The power values for the inlet and ideal sections were constant throughout the range of submergence levels; an expected result since only the lower water level was varied in these simulations. Variations in the lower water level mean that each simulation has varying hydraulic potential energy, so further processing was required to compare the results, as shown in the following section. Note that [figure 4](#) does not show data for submergence levels of $\psi_L = 0.9$ or 1.0 ; this was because of domain geometry. For a rotational, dynamic mesh, it was easiest to fully enclose the cylindrical screw trough. In reality, the screw trough is only enclosed for three quarters of its circumference, with the top open to atmosphere. In the simulation, when submergence levels reached 90% and 100%, the lower end of the screw was sealed with the fully enclosed trough and water surface. That created an air pocket that seemed to

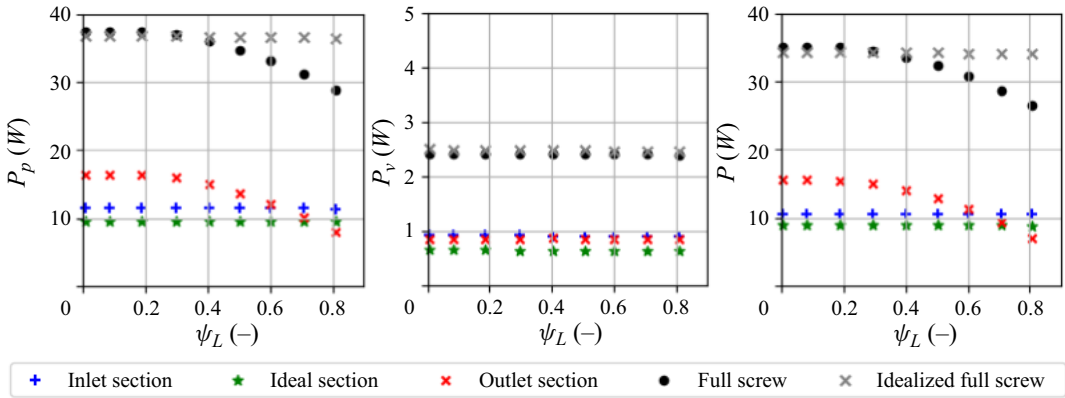


Figure 4. Power and its components (static and viscous pressure, P_p and P_v , respectively) in panels with respect to outlet submergence. Results are from screw 2 (cf. table 3). Each plot shows power of the inlet, ideal and outlet sections as well as the full screw power and ideal full screw power.

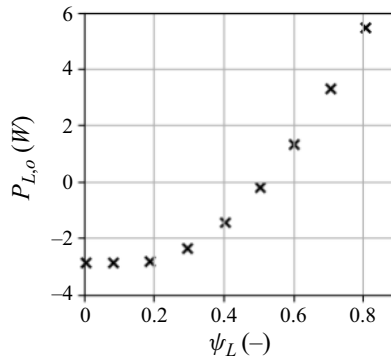


Figure 5. Outlet loss calculated with (1.6) for the range of submergence values for screw 2.

cause backpressures that significantly impacted the flow dynamics in the first few buckets of the screw. Effectively, this caused the system to transition from open channel flow to a complex, partially filled pipe flow.

Since a screw generator is an array of translating buckets, it seemed reasonable to scale the ideal section by the length ratio (S/L) to find the ideal power production of the full screw. This gave very reasonable results since it yielded slightly higher power values than the actual total, and the results did not seem to be impacted by varying lower water levels. The consistency of the scaled ideal screw power indicated that the simulated screw was long enough that its ideal section was effectively free of inlet and outlet effects.

Since the ideal section seemed to be free from outlet effects, it was used to quantify the outlet power loss ($P_{L,o}$) using the following relationship:

$$P_{L,o} = \frac{L_o}{L_{id}} P_{id} - P_o, \tag{3.1}$$

where $P_{L,o}$ is the outlet power loss, L_o is the outlet section length, $L_{id} = S$ is the ideal section length, P_{id} is the ideal section power and P_o is the outlet section power.

An example of the outlet power loss is shown in figure 5 for the results of figure 4. The outlet power loss represents power loss due to phenomena specifically at the screw outlet.

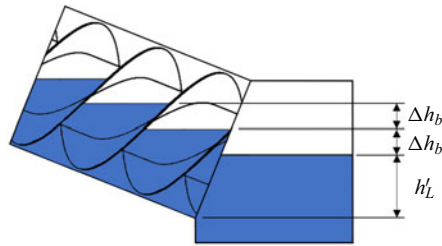


Figure 6. An ASG just before the final bucket begins to empty into the lower basin. The optimal lower water level and a local bucket head drop are shown in dimensional terms.

After this preliminary analysis, the authors decided that more data were required to quantify the effects that varying fill height, inclination angle and number of blades had on outlet power loss in ASGs. It was also determined that screws 4 and 5 were both excellent representations of ASG performance in all full-scale screws (i.e. all screws other than screws 1 and 2 – the laboratory-scale screws). So, screw 4 was simulated across the range of submergences with $N = 3, 4$ and 5 blades. Screw 4 was also used to examine the effects of inclination angle on power loss. Inclination angle was varied from $\beta = 15^\circ$ to 35° by increments of 5° ; this range included the most common inclination angle for installed ASG powerplants, $\beta = 22^\circ$ (Lashofer 2018). Since it was already running for a parallel study, screw 5 was used to simulate the effects of varying fill height on outlet power loss. The fill ratio was varied from $f = 0.5$ to 1.3 by increments of 0.1. Results of these simulations are presented in figures 7 to 11 and were used for the model development presented in this article.

3.2. Model development

To reiterate, the initial simulations (cf. figure 4, table 3) were run with a constant fill height ($f = 1$), inclination angle ($\beta = 24.5^\circ$) and number of blades ($N = 3$); subsequent simulations varied these parameters. To allow for direct comparisons across the range of simulations, the outlet submergence was first normalized. The difference between the optimal submergence was used for normalization. However, the optimal lower water level described by Nuernbergk (1.5) is only valid when fill heights are $f = 1$. Since some of the data gathered in this study varied fill height, a new optimal submergence level treatment was first developed before further analysis began.

In theory, at the optimal lower submergence, the outlet of the screw provides a similar amount of backpressure in its last buckets of the screw such that they operate like a bucket within the ideal section of the screw. For context, the optimal lower water level and head drop between buckets (Δh_b) are shown in figure 6.

Gap flow caused screw buckets to exhibit minor drainage earlier than the screw outlet; however, most of the bucket volume drains as the blades move to a position below the free surface of water at the screw outlet. So, the ideal lower water level can be found when the blade is at its last position before it drops beneath the fill height of the final bucket. When the blade is in this position, the head drop between the last bucket and lower basin water levels should be equal to the bucket head drop (Δh_b).

The presence of a non-zero lower water level had a few benefits during operation. It allowed backpressures to remain relatively consistent through bucket transport through the screw. It also prevented early drainage of screw buckets since the gap flow was more consistent. Finally, it prevented backfilling since the lower basin water level was lower than the last bucket height; water was prevented from spilling from the lower basin into the last bucket at the outlet.

Informed by these observations, the following equation was developed to estimate optimal lower submergence (i.e. the dimensionless optimal lower water level). Effectively, the bucket head drop was found for any bucket fill height and corresponding screw geometry. It was used to find the

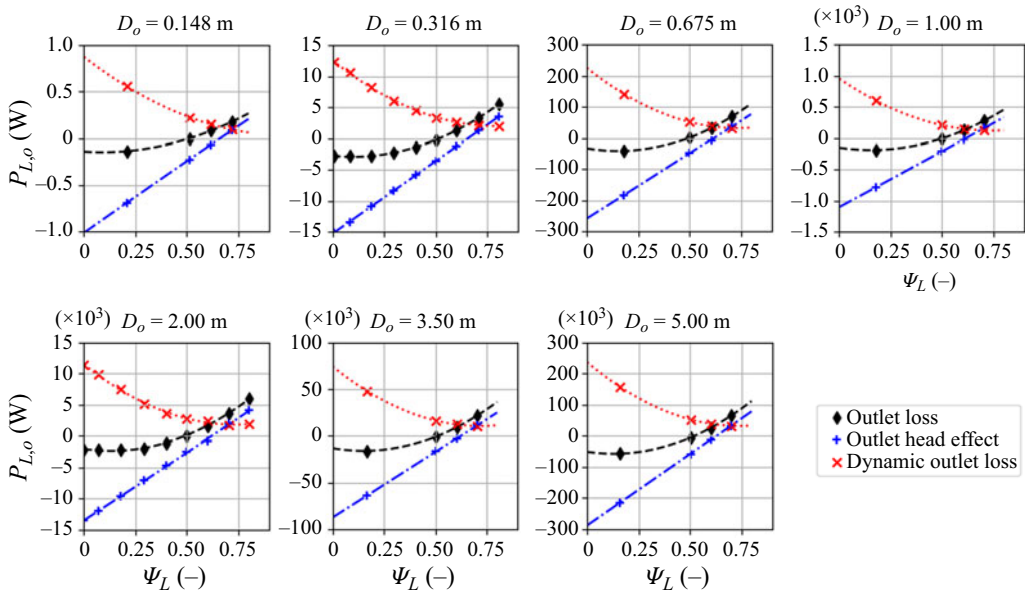


Figure 7. Effects of varying lower submergence on outlet power loss – and its two components – for the seven simulated ASG length scales.

corresponding lower water level

$$\psi'_L = \frac{1}{D_o \cos \beta} \left[\left(\frac{S}{2} - \frac{S}{N} \right) \sin \beta + z_{wl} - z_{min} \right]. \tag{3.2}$$

With a new, more general optimal lower water level relationship, the outlet power loss model could be further developed. Outlet power loss was separated into two components: outlet head effect (P_{oh}) and dynamic outlet loss ($P_{L,od}$). Total outlet power loss was then written as

$$P_{L,o} = P_{oh} + P_{L,od}. \tag{3.3}$$

The outlet head effect was developed with first principles. It was proposed as the magnitude of hydrostatic pressure present when the lower water level was above or below optimal submergence. When water levels were lower than optimal submergence, outlet head effect was negative; in this case, the outlet would be considered under-submerged (i.e. $\psi_L < \psi'_L$). This parameter accounts for variations in hydraulic potential between the simulations.

Outlet head effect was written as

$$P_{oh} = \rho g Q D_o (\psi_L - \psi'_L) \cos \beta. \tag{3.4}$$

Dynamic outlet power loss was defined as the difference between total outlet loss measured in the simulations ($P_{L,o}$) and the outlet head effect. It was defined by rearranging (3.2) as

$$P_{L,od} = P_{L,o} - P_{oh}. \tag{3.5}$$

All length-scale simulations (cf. table 3) were compared in figure 7. In the figure, submergence levels were normalized by the optimal submergence such that an x -axis value of $\psi_L - \psi'_L = 0$ would correspond to the optimal submergence. Screw diameter (i.e. length scale) is indicated in the panel titles. Each panel compares outlet power loss, and its two components, for the range of lower submergences.

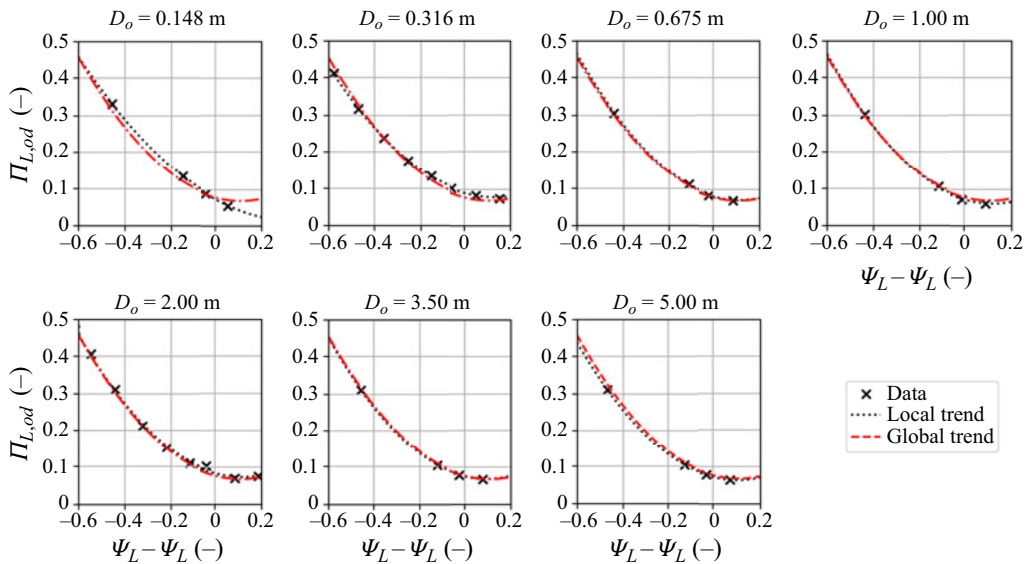


Figure 8. Impact of normalized outlet submergence on dimensionless dynamic outlet loss. Results shown with a local trendline and a global trendline (based on screws 3 to 7 results) to aide in visualizations and comparisons.

Trendlines were fit to the data to improve readability and illustrate the seemingly predictable nature of system behaviours.

The results of figure 7 suggest that dynamic outlet power loss may be approximated with a second-order polynomial fit to a high degree of accuracy. Theoretically, this relationship seemed reasonable since the dynamic outlet power loss would be expected to vary with the wetted area of blades in the outlet region; an attribute that scales to the second order of outlet water level.

Analysing outlet power loss in components seemed advantageous since it allowed one component to be modelled with first principles. Additionally, it helped normalize data before modelling: the outlet power loss varied from positive to negative, where the dynamic outlet loss was always positive. Dynamic outlet loss was much more suitable for empirical fitting since its always-positive nature added stability benefits to the final model.

A similarity study and dimensional analysis were conducted to allow direct comparisons between each length-scale screw with respect to outlet submergence. Dimensionless dynamic outlet loss was written as

$$\Pi_{L,od} = \frac{P_{L,od}}{\rho g D_o Q}. \quad (3.6)$$

Figure 7 was recast as the dimensionless dynamic outlet power loss on the y-axis (figure 8). To aide visualization, a local second-order polynomial trendline was fit to the dynamic outlet loss for each length-scale simulation set. A global trendline was also fit to the datapoints. The global trendline was fit to the full-scale ASGs (screws 3 to 7) since they were the practical, powerplant-sized screws and seemed to yield very consistent results compared with each other. The laboratory-scale screws (screws 1 and 2) appeared to exhibit slight deviation from the global trendline. The results seemed reasonable since laboratory-scale screws would be proportionally more impacted by losses like viscous drag.

The global quadratic trend applied across the dataset seemed to effectively approximate dynamic outlet loss for all scale-sized screws. It seemed to have very high accuracy in full-scale screws (i.e. $D_o = 0.675$ to 5 m), and maintained reasonable accuracies for the laboratory-scale simulations (i.e. $D_o = 0.148$ and 0.316 m). The smallest laboratory screw seemed to deviate from the global trend in cases of non-optimal submergence, with the largest deviation for higher than optimal submergences. The larger

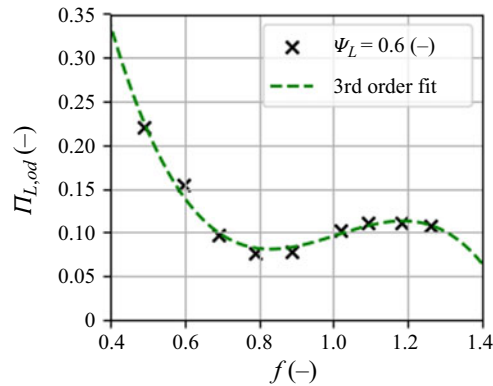


Figure 9. Effects of varying fill height on dimensionless dynamic outlet power loss for screw 5.

laboratory-scale screw ($D_o = 0.316$ m) exhibited similar deviation only in cases of low submergence levels. Altogether, it is suggested that the dimensional analysis was successful in normalizing the scaling effects seen in the dimensional data. It yielded a reasonable universal fit for all scale-sized screws. The universal dynamic outlet loss fit performed particularly well when predicting outlet power loss in practical, full-scale ASGs.

3.3. Correction terms

Figure 8 was created from data with constant fill height, inclination angle and number of blades. So, additional simulations were conducted to quantify the impacts of varying these parameters.

3.3.1. Fill height

The impact of fill height on dimensionless dynamic outlet power loss was investigated first. The results of the fill height simulations are shown in figure 8. Simulations were performed on screw 5 with an outlet submergence level of $\psi_L = 0.6$. Fill height can be varied by either maintaining flow rate and adjusting rotation speed, or maintaining rotation speed and adjusting flow rate. To better observe the impact fill height had on dynamic outlet power loss, rotation speed was maintained. So, the flow rate was varied to set fill height in this simulation set.

The volume of water in the screw buckets effectively varied to the third power of bucket height. A third-order polynomial trendline was fit to the data. The polynomial seemed to be a reasonably accurate approximation, which suggested that the dynamic outlet power loss scaled with volume of water discharging from the buckets at the outlet. This seemed reasonable since dynamic effects like drainage or backfilling at the outlet were impacted by variations in flow rate and flow rate scales to the third power of height (length scale). The third-order fit from figure 9 yields the following equation:

$$\Pi_{L,od(f)} = -1.449f^3 + 4.378f^2 - 4.292f + 1.444. \quad (3.7)$$

The fill height relationship in (3.7) was normalized with respect to a fill height of $f = 1$ since that is usually the target nominal fill height. So, the (3.7) relationship was divided by itself evaluated at $f = 1$, and recast as the fill height correction term (λ_f)

$$\lambda_f = \frac{\Pi_{L,od(f)}}{\Pi_{L,od(f=1)}} = \frac{-1.449f^3 + 4.378f^2 - 4.292f + 1.444}{0.08100}. \quad (3.8)$$

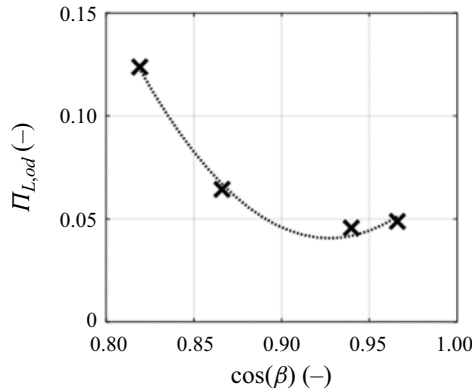


Figure 10. Effect of varying inclination angle on dimensionless dynamic outlet power loss for screw 4.

3.3.2. Inclination angle

A similar process was carried out to quantify the impact of inclination angle on dynamic outlet power loss. Screw 4 was simulated across a range of inclination angles to observe its impacts. Fill height was maintained at $f = 1$ for all simulations; all other parameters were kept consistent with screw 4 in table 3. To maintain stability, the x -axis of figure 10 was set as the cosine of the inclination angle to prevent x -axis values exceeding a magnitude of unity.

Inclination angle had a notable impact on the dynamic outlet power loss. It seemed to be approximated with reasonable accuracy by a second-order polynomial fit. Interestingly, the minimum point of the quadratic fit function (the point corresponding to the least dynamic outlet loss) was at an inclination angle of approximately $\beta = 22^\circ$, which is the most common inclination angle in real, full-scale screw generator powerplants. The second-order trendline had the following form:

$$\Pi_{L,od(\beta)} = -2.3267 \cos^2 \beta + 4.2921 \cos \beta - 1.9305. \tag{3.9}$$

Similarly to the fill height correction term, this relationship was centred around the minimum dynamic outlet power loss to normalize the results and develop the correction term

$$\lambda_\beta = \frac{\Pi_{L,od(\beta)}}{\Pi_{L,od(\beta=22^\circ)}} = \frac{-2.3267 \cos^2 \beta + 4.2921 \cos \beta - 1.9305}{-0.04887}. \tag{3.10}$$

3.3.3. Number of blades

The number of blades was varied in screw 4 to determine its impact on the dynamic outlet power loss. Results are shown in figure 11 plotted alongside the global fit from figure 8. All parameters were kept consistent with the initial runs of screw 4 (cf. table 3), except the number of blades was varied between $N = 3, 4$ and 5 – the most practical range for the number of blades. Screws with $N = 1$ or 2 blades are not practical for hydropower systems since they tend to underfill during operation and operate with lower efficiencies. Screws with $N \geq 6$ blades are also uncommon since the added friction associated with the additional blade surfaces outweighs any practical gains in power production. So, practically, but with some exceptions, screw generators have been installed with $N = 3, 4$ or 5 blades (Lashofer 2018).

The second-order local fit of each panel varied in curvature, magnitude and y -intercept location. It was determined that a treatment was required to model dynamic outlet loss with respect to a varying number of blades. Due to the discrete nature of this design parameter, it was necessary to generate individual curve-based fits for each number of blades. Altogether, the proposed form of the dimensionless dynamic

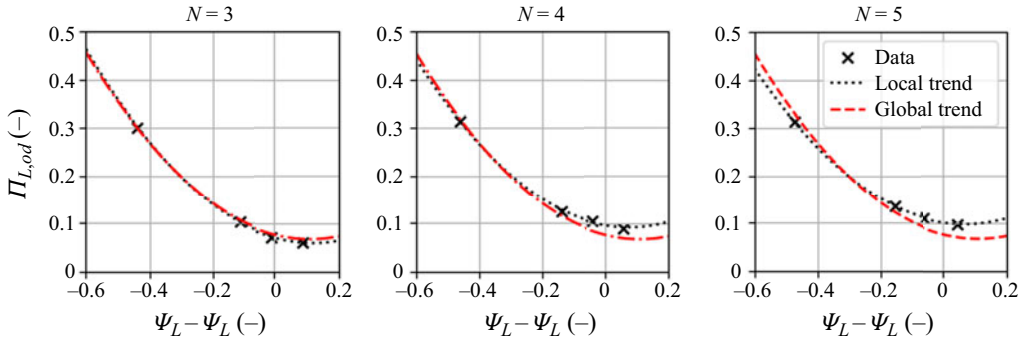


Figure 11. Impact of varying number of blades and submergence on dimensionless dynamic outlet power loss.

outlet loss takes the following conditional form:

$$\Pi_{L,od} = \begin{cases} 0.8373(\psi_L - \psi'_L)^2 - 0.2069(\psi_L - \psi'_L) + 0.06244, & N = 3, \\ 0.8520(\psi_L - \psi'_L)^2 - 0.1327(\psi_L - \psi'_L) + 0.09344, & N = 4, \\ 0.8268(\psi_L - \psi'_L)^2 - 0.1131(\psi_L - \psi'_L) + 0.1002, & N = 5. \end{cases} \quad (3.11)$$

Since all correction factors were developed by isolating variations to individual parameters and resulting relationships yielded single correction factors, the principle of linear superposition was used to combine all relationships and define a single equation for the dynamic outlet power loss

$$P_{L,od} = \frac{\rho g Q D_o}{\lambda_f \lambda_\beta} \Pi_{L,od}. \quad (3.12)$$

The total outlet loss (3.3) can then be written as the sum of the dynamic outlet loss (3.12) and the outlet head effect (3.4)

$$P_{L,o} = \rho g Q D_o \left(\frac{\Pi_{L,od}}{\lambda_f \lambda_\beta} + (\psi_L - \psi'_L) \cos \beta \right). \quad (3.13)$$

This system of equations yields a practical outlet power loss model that can be implemented with the following algorithm.

- (i) Calculate dimensionless dynamic outlet loss for a given lower water level using (3.11).
- (ii) Calculate the fill height correction factor with (3.8).
- (iii) Calculate the inclination angle correction factor with (3.10).
- (iv) Calculate the outlet loss with (3.13). If outlet power loss components are required, use (3.4) to estimate outlet head effect and (3.12) to estimate dynamic outlet loss.

After using simplifications to produce (3.12), the model was more straightforward to implement. This model (hereafter the ‘proposed model’) was compared with the current outlet power loss model presented by Kozyn & Lubitz (2017) (hereafter the ‘Kozyn model’).

3.4. Model evaluation

Given the challenges associated with directly measuring outlet loss in an operating ASG, it was imperative to compare model predictions by applying them to a full-scale performance prediction model. The Kozyn model was applied as a built-in update to the original Lubitz model (Lubitz *et al.* 2014; Kozyn & Lubitz 2017). So, the proposed outlet loss model defined in the previous section was applied as an update to the Lubitz model as well.

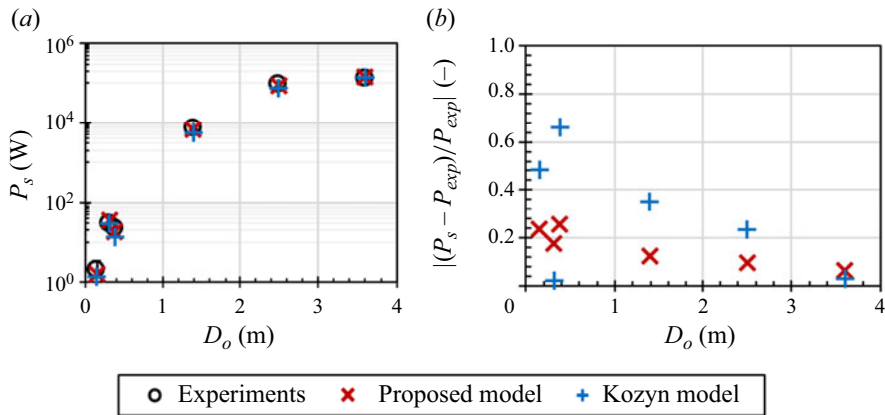


Figure 12. Comparison between proposed model, Kozyn model and experimental data from laboratory-scale and full-scale screw generators. Shaft power is compared across a range of outer diameters (a) and the absolute error with respect to experimental datapoints are compared as well (b). $R^2 = 0.990$ (proposed model) and $R^2 = 0.910$ (Kozyn model).

The mechanical power generated (termed ‘shaft power’, P_s) is described as the product of torque and rotation speed transmitted by the screw shaft into the gearbox/generator assembly. The full Lubitz model was run with both the Kozyn model and proposed model outlet loss corrections applied and the resulting shaft power predictions were compared between the models and experimental data. Experimental datapoints were gathered from laboratory experiments and field measurements that had a wide range of length scales. A log plot was used so data could be more easily visualized on the same plot. The absolute error between model predictions and the experimental data was plotted as well to aide in observations and evaluations (figure 12).

The experimental measurements for shaft power had a measurement uncertainty between 3.3 % and 7.4 % for the range of scale measurements used in this analysis and evaluation (Simmons *et al.* 2021). The proposed model had a coefficient of determination of $R^2 = 0.990$, and the Kozyn model $R^2 = 0.910$ when compared with the data. The proposed model consistently demonstrated higher accuracy for all screws; it yielded improvements between 1.7 % and 20.4 % to model prediction accuracy. The Kozyn model tended to overestimate outlet losses, especially in cases of sub-optimal submergence. To more robustly assess model performance, the models were used to predict performance across multiple screw generator datasets, including data from the Ruswarp, Buckfast and Waterford powerplants as well as in the laboratory. The Ruswarp powerplant comparison is shown in figure 13; all other comparisons are shown in the supplementary material for brevity.

Both models demonstrated reasonable accuracy across all scenarios. The Kozyn model had coefficients of determination of $R^2 = 0.529, 0.945, 0.946, 0.062$ and 0.746 with data from respective figures in this article’s supplementary material document. When the performance model was updated to use the proposed outlet power loss model presented in this paper, the coefficients of determination became $R^2 = 0.928, 0.967, 0.537, 0.131$ and 0.961 for the same respective range. Generally, the proposed model yielded overall performance prediction model accuracy once implemented.

While the proposed model was based on a comprehensive range of simulated data that spanned multiple length scales, its accuracy lessened for normalized submergence levels above 0.2 (over-submerged outlets). Some tested datapoints extended beyond training conditions, so the model was extrapolating to predict performance. The Kozyn model was only validated against a robust set of laboratory-scale data and the data from the Waterford screw generator powerplant (cf. supplementary figures). Neither model was expected to be highly accurate for the Buckfast or Ruswarp screw data considering the differences in scale between the powerplants. However, it is important to note that the Kozyn model was trained

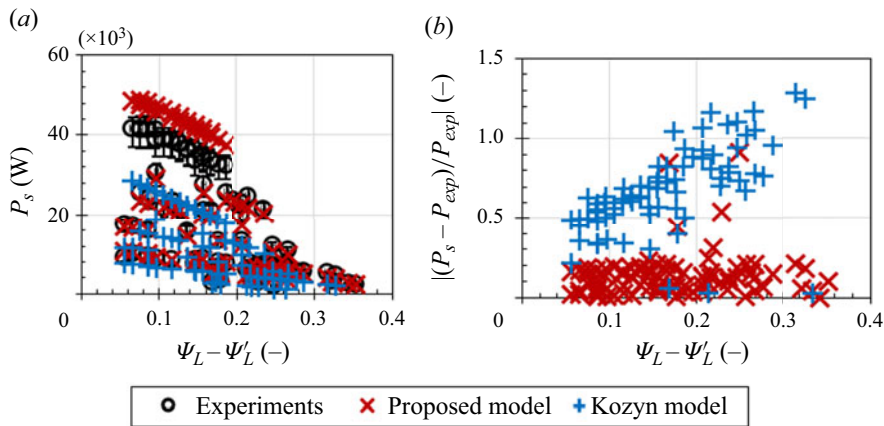


Figure 13. Ruswarp screw generator powerplant experimental data compared with both proposed ($R^2=0.928$) and Kozyn models ($R^2=0.529$). Shaft power is compared across a range of normalized outlet submergence (a) as well as absolute error (b).

with the Waterford powerplant data and data collected from screw 2 (which is of a similar scale to screw 15). Hence, for these screws, the Kozyn model was expected to exhibit artificially high agreement. The comparisons are still shown since they help to evaluate and visualize the accuracy of the proposed model.

The Kozyn model appeared to diminish in accuracy when applied to real-world, full-scale screw generator installations. The proposed model demonstrated reasonable accuracy improvements. It consistently forecasted greater power loss as submergence levels rose; a phenomenon that was observed in real screw installations with flooded outlets. So, it seemed the proposed model was able to perform well, even when extrapolating beyond its training range.

The proposed model exhibited superior performance when submergence levels were lower than optimal. Performance improvements were not as drastic for high submergence levels. It is noted that the Waterford powerplant is unique since it is fully enclosed for year-round operation in a cold climate. To enclose the screw at its outlet, an airlock curtain is installed to seal the outlet of the screw; it penetrates into the water at the outlet similarly to a sluice gate. The airlock may have influenced the outlet fluid dynamics since outflow must traverse under the curtain before returning to the main waterway, potentially altering the dynamic outlet losses when compared with an open-air screw. Nevertheless, the proposed model seemed to perform reasonably well overall with a higher margin of error in excessive submergences.

Observing the Ruswarp data comparisons (figure 13), there was a marked improvement in shaft power prediction accuracy with the proposed outlet power loss model implemented. Despite all data occupying the over-submerged range, the proposed model achieved higher accuracy for almost every datapoint. It yielded absolute errors of 5% or less in 26.25% of datapoints, and 10% or less in 48.75% of datapoints. The proposed model predicted power with approximately 13.68% margin of error compared with the nominal experimental data. In comparison, the Kozyn model exhibited 5% or less error in 1.25% of the datapoints, and 10% or less error in those same 1.25% of datapoints. Altogether, the Kozyn model had an average absolute error of 42.55% compared with the experimental data. So, the proposed model achieved an accuracy improve of 28.87% for the Ruswarp powerplant performance predictions.

The proposed model predicted similar outlet power loss levels as the Kozyn model for the laboratory-scale screw (cf. supplementary figures). While the proposed model demonstrated greater accuracy in under-submerged cases, the Kozyn model was more accurate in highly over-submerged scenarios. This pattern mirrored the comparisons between local and global fits illustrated in figure 13. Specifically, the accuracy of laboratory-scale screw outlet power loss predictions diminished when normalized submergence levels exceeded $\psi_L - \psi'_L > 0.1$, or fell below $\psi_L - \psi'_L < -0.3$ (cf. figure 13). The

results suggest potential accuracy issues with the proposed outlet power loss models when applied to very small screw generators. So, although the proposed outlet power loss model demonstrates broad prediction accuracy improvements, it should be used with caution when applied to pico-scale ASGs.

4. Conclusion

This study presented a new outlet power loss prediction model for ASGs. The proposed model is a drop-in replacement for existing performance prediction models. The proposed model offered notably enhanced accuracy when compared with the state-of-the-art outlet power loss model presented by Kozyn & Lubitz (2017). It yielded the highest increase in prediction accuracy for real, full-scale ASG powerplants.

The proposed model and the Kozyn model for outlet power loss were evaluated and compared against experimental data collected from laboratory screw generators and powerplants. While the Kozyn model appeared effective in predicting performance in laboratory-scale screws and the smaller Waterford powerplant, it had not yet been evaluated against medium to large screw generator powerplants. The comparisons drawn in this study suggest that the proposed model offers substantial accuracy improvements, especially when predicting outlet power loss in real, full-scale ASG powerplants. Since the proposed model was developed using simulated data collected from ASGs ranging from $D_o = 0.15$ to 5 m, it is implicitly more universal. The proposed model saw large accuracy improvements, particularly on real-world screws within normal operating bands. However, analysis has demonstrated that the proposed model has accuracy issues when predicting outlet power loss for pico-scale (laboratory-scale) screw generators that are over-submerged, or highly under-submerged.

The introduction of these data and the newly developed outlet power loss model to the literature can significantly enhance performance prediction accuracy for ASGs. Integrating this new model into optimization software will help refine the site-specific design of screw generators to yield higher efficiencies and returns on investment. The novel analysis and data presented in this article also serve as a foundation for ongoing model refinement, enhancement and evaluation.

Acknowledgments. The authors gratefully acknowledge the efforts of T. Bouk and B. Weber of GreenBug Energy Inc. (Canada) and Dr G. Dellinger of ENGEES (France) for their continued support. The authors gratefully acknowledge the help and support of A. Clayton, D. Mann and S. Moore of Mann Power Hydro Ltd. for granting site access, sharing data and helping with surveying and measurements. We are also very grateful to M. Ford, C. Mather, R. Newman, S. Larkin, D. Moore and the rest of the team at Whitby Esk Energy, for their help and support with surveying and measurements at Ruswarp Hydro. The assistance of C. Elliott (On Stream Energy Ltd.) and the Buckfast Abbey staff was integral to the measurements taken at Buckfast Abbey's Hydro plant and is greatly appreciated. The authors would also like to thank D. Dechambeau of Southeast Power Engineering for his insights, and his help and support with surveying and measurements of the Romney Weir ASG plant in Windsor, UK.

Funding statement. This research was supported by grants from the Natural Science and Engineering Research Council (NSERC) of Canada, Collaborative Research and Development (CFD) program grants CRDPJ 433740-12 and CRDPJ 513923-17.

Competing interests. None.

Data availability statement. Some replication data and code available upon request.

Ethical standards. The research meets all ethical guidelines, including adherence to the legal requirements of the study country.

Author contributions. Conceptualization: S.S; W.D.L. Methodology: S.S; W.D.L. Data curation: S.S; W.D.L. Data visualization: S.S; W.D.L. Writing original draft: S.S; W.D.L. All authors approved the final submitted draft.

Supplementary material. Supplementary material is available at <https://doi.org/10.1017/flo.2024.29>.

References

- AIGNER, D. 2008 *Überfälle*. Dresdner Wasserbauliche Mitteilungen.
- DALLEY, S. & OLESON, J.P. 2003 Sennacherib, Archimedes, and the water screw: the context of invention in the ancient world. *Technol. Culture* **44** (1), 1–26.
- FERGNANI, N., SILVA, P. & BAVERA, D. 2017 Efficiency assessment of a commercial size Archimedean screw turbine based on experimental data. *Hydro 2017*, Seville, Spain.

- KOZYN, A. 2016 *Power Loss Model for Archimedes Screw Turbines*. University of Guelph.
- KOZYN, A. & LUBITZ, W.D. 2017 A power loss model for Archimedes screw generators. *Renew. Energy* **108**, 260–273.
- LASHOFER, A. (2018). Projekt Wasserkraftschnecken Verortung. Available at: <https://www.lashofer.at/deutsch/wasserkraftschnecke/projekt-wasserkraftschnecken-verortung/>
- LUBITZ, W. D. (2014). *Gap Flow in Archimedes Screws*. CSME International Congress.
- LUBITZ, W.D., LYONS, M. & SIMMONS, S.C. 2014 Performance model of Archimedes screw hydro turbines with variable fill level. *J. Hydraul. Engng* **140** (10), 04014050.
- LYONS, M. 2014 *Lab Testing and Modeling of Archimedes Screw Turbines*. University of Guelph.
- NUERNBERGK, D.M. 2020 *Wasserkraftschnecken: Berechnung und Optimaler Entwurf von Archimedischen Schnecken als Wasserkraftmaschine [Hydropower Screws: Calculation and Design of Archimedes Screws for Hydropower]*, 2 edn. Verlag Moritz Schäfer.
- NUERNBERGK, D.M. & RORRES, C. 2013 Analytical model for water inflow of an Archimedes screw used in hydropower generation. *J. Hydraul. Engng* **139** (2), 213–220.
- RORRES, C. 2000 The turn of the screw: optimal design of an Archimedes screw. *J. Hydraul. Engng* **126** (1), 72–80.
- SIMMONS, S.C. 2018 *A Computational Fluid Dynamic Analysis of Archimedes Screw Generators*. University of Guelph.
- SIMMONS, S.C., DELLINGER, G. & LUBITZ, W.D. 2023 Effects of parameter scaling on archimedes screw generator performance. *Energies* **16** (21), 1–22.
- SIMMONS, S.C., ELLIOTT, C., FORD, M., CLAYTON, A. & LUBITZ, W.D. 2021 Archimedes screw generator powerplant assessment and field measurement campaign. *Energy Sustain. Dev.* **61**, 144–161.
- SIMMONS, S.C. & LUBITZ, W.D. 2020 Analysis of internal fluid motion in an Archimedes screw using computational fluid mechanics. *J. Hydraul. Res.* **59** (6), 1–15.
- SIMMONS, S.C. & LUBITZ, W.D. 2021 Archimedes screw generators for sustainable micro-hydropower production. *Intl J. Energy Res.* **45** (12), 17480–17501.
- SIMMONS, S.C. & LUBITZ, W.D. 2022 *An Updated Model for Gap Leakage in Archimedes Screw Generators*. CSME International Congress.
- SONGIN, K.J. & LUBITZ, W.D. 2019 Measurement of fill level and effects of overflow in power-generating Archimedes screws. *J. Hydraul. Res.* **57** (5), 1–12.